Originally published 29 July 2010; corrected 5 October 2010

www.sciencemag.org/cgi/content/full/science.1191184/DC1

Supporting Online Material for

A Planar Cell Polarity Protein Governs Collective Cell Movement and Ciliogenesis via the Septin Cytoskeleton

Su Kyoung Kim, Asako Shindo, Tae Joo Park, Edwin C. Oh, Srimoyee Ghosh, Ryan S. Gray, Richard A. Lewis, Colin A. Johnson, Tania Attie-Bittach, Nicholas Katsanis, John B. Wallingford*

*To whom correspondence should be addressed. E-mail: wallingford@mail.utexas.edu

Published 29 July 2010 on *Science* Express
DOI: 10.1126/science.1191184

This PDF file includes

Materials and Methods
Figs. S1 to S10
References

Other Supporting Online Material for this manuscript includes the following:
(available at www.sciencemag.org/cgi/content/full/science.1191184/DC1)

Movies S1 to S4

Correction 5 October 2010: An early version of the SOM was posted in error. This is the correct SOM with 10 figures.

Supporting Online Materials

Supplemental Materials and Methods

Xenopus embryo manipulations:

Ovulation was induced in *Xenopus laevis* adult females by injection of human chorionic gonadotropin. The next day, eggs were squeezed, fertilized *in vitro* and dejellied in 3% cysteine (pH 7.9) at the two-cell stage. Fertilized embryos were washed and subsequently reared in 1/3X Marc's modified Ringer's (MMR) solution. For microinjections, embryos were placed in a 2% ficoll in 1/3X MMR solution, injected using forceps and an Oxford universal micromanipulator, and reared in 1/3X MMR solution containing 2% ficoll to stage 9. Injected embryos were washed and grown in 1/3X MMR alone. For rescue experiments, embryos at stage 12 were fixed in MEMFA to measure the area of the blastopore. The area of blastopore was measured by drawing lines along the boundary of the blastopore using Image ProPlus. *In situ* hybridization was performed as described (*1*).

Cloning, plasmids, MO and antibodies:

The *Xenopus* homologue of *Drosophila* Fritz was identified by searching NCBI database (Accession number: BC108509). The Fritz ORF was amplified by PCR and cloned into pCS107GFP-3STOP, pCS107Myc-3STOP or pCS107Flag-His-3STOP. Septin 2 (Accession number: AF212298) and septin 7 (Accession number: BC074298) cDNAs were identified in Xenbase and obtained from the I.M.A.G.E consortium and the ORF of septin 2 and septin 7 were amplified by PCR and subcloned into pCS107Myc-3STOP and pCS107GFP-3STOP. Translation-blocking morpholino-oligonucleotides (MO) were designed to be complementary to the translation start site and MOs were made from GeneTools. Sequences of MOs are as follows: Fritz-MO sequence: 5'-ACAGCTCAGTCAGACAAAACGACAT-3', Septin 2-MO sequence: 5'-TAAACTGAGCCTGTTGCTTTGACAT-3' and Septin 7-MO sequence: 5'-TGCTGTAGAGTCAGTGCCTCGCCTT3'. A Fritz antibody was generated by OPEN Biosystems from the following peptide sequence: KKINSPDINRQLDK. The anti-Septin 2 antibody was a gift from E. Spiliotis. The following antibodies were purchased: anti-Septin 7 [Santa Cruz (sc-20620)], anti-α tubulin [Sigma (T9026)], anti-γ tubulin [Abcam (ab27076)], anti-Myc [Abcam (ab9106)], anti-Flag [Abcam (ab21536)], and anti-GFP [Abcam (ab6556).

Morpholino-oligonucleotide and mRNA injections:

Capped mRNA was synthesized using mMessage mMachine kits (Ambion). mRNA or antisense MO was injected into two ventral blastomeres to target the epidermis, into two dorsal blastomeres to target dorsal marginal zone, or into all four blastomeres at the four-cell stage to generate protein lysates (*2*). Fritz MO was injected at 30~35 ng per blastomere. Septin 2-MO and Septin 7-MO were injected each 40 ng per blastomere and various amounts of mRNAs were injected.

Blastopore size measurement:

The image of the blastopore side of the wild type and MO-injected embryos were taken using a stereomicroscope, and the area of the blastopore was measured by drawing lines along the boundary of the blastopore using ImageProPlus. Statistical cmparisons were performed using the Mann Whiteny U test.

Imaging of Keller explants:

GFP-septin2 (10pg / blastomere) and membrane RFP (50pg /blastomere) or GFP-Fritz (30pg /blastomere) were injected at the dorsal site of 4 cell stage and the dorsal marginal zone tissues were dissected out at stage10.5 using forceps and eyebrow hair knives. Each DMZ was mounted to a fibronectin-coated dish in Steinberg's solution to be observed by confocal microscopy. For the time-lapse imaging of membrane dynamics, Fritz-MO (20-30ng / blastomere) or septin-MO (40ng / blastomere) was injected with membrane-RFP and time-lapse images were taken every 10 seconds for 5-6min at stages indicated. For L/W ratio and cell orientation measurements, the outline of each DMZ cell was drawn using Image ProPlus and the length and width in addition to the angle of the long axis, of each cell were measured. Statistical tests (as specified in Fig. S3) were performed with GraphPad Instat software; Circular statistics and rose diagrams were generated using Oriana Software.

Confocal Image quantification:

For cortical septin localization, pixel intensity plots were collected across cells, "cortical" septin was defined as the mean sept2-GFP signal along the intensity plot line and within 0.5 μm of the cell membrane (defined as the peak of signal for co-expressed membrane-RFP). We defined "cytoplasmic" septin localization as the mean sept2-GFP signal along intensity plot line through the cell but not within the defined "cortical" domain. We then compared the ratio of cortical to cytoplasmic sept2-GFP signal for controls versus morphants.

Area and pixel Heterogeneity of Sept7 foci was measured using ImageProPlus. Heterogeneity was defined as the fraction of pixels within each structure that differ by more than 10% from the average pixel intensity for that structure. Statistical comparisons were made using the Mann-Whitney U test.

Immunostaining and confocal imaging:

Immuostaining was performed as previously described (*3*). For ciliary epidermal staining, embryos were fixed in 1X MEMFA for 2 hours at room temperature at stage 26~27, washed with PBST (PBS plus 0.1% Triton X-100) and blocked for 30 min at RT in 10% FBS and 5% DMSO in PBST. We incubated the embryos with primary antibodies diluted in blocking solution at 4°C overnight. The following primary antibodies were used: anti-Sept 2 (1:50 dilution), anti-Sept 7 (1:50), anti-Fritz (1:50), anti-γ tubulin (1:500), anti-α tubulin (1:1,000) and anti-Myc antibody (1:300). After washing five times with PBST for over an 1 hour, primary antibodies were detected with Alexa Fluor-488 or 555 goat anti-rabbit or mouse immunoglobulin (IgG) diluted in the blocking solution. For basal body staining, embryos were fixed in Dent's solution (20% DMSO in methanol) at -20° C

overnight, washed and incubated in methanol at -20° C overnight. The embryos were gradually rinsed through methanol: Ptw (PBS plus 0.1% Tween; 3:1, 1:1, 1:3) into Ptw. After immunostaining, the embryos were imaged in TBST on an inverted Zeiss LSM5 Pascal confocal microscope. Confocal images were processed and cropped in Imaris software (BITPLANE scientific solutions), then Adobe Illustrator and Adobe Photoshop were used for compilation of figures.

Co-immunoprecipitation (IP) and immunoblot assay:

Tagged proteins were expressed by mRNA injection (300 pg into each blastomere at the four-cell stage) and embryos were reared in 1/3X MMR until stage 23~24. The embryos were lysed in TBSTG (TBS+0.1% Triton-X100, 5% glycerol) containing a protease inhibitor cocktail (Sigma). The lysates were centrifuged for 15 min at 14,000 rpm at 4℃ and the supernatants were saved and incubated with anti-myc antibody conjugated beads (Abcam). The beads were rinsed in TBSTG and eluted using 1X SDS sample buffer. The elutes were analyzed by SDS-PAGE and protein blot analysis using anti-GFP antibody. For reciprocal IP, anti-Myc conjugated beads (Abcam) were used to pull down Myc-Septin 2 and the beads were washed and eluted using the 1X SDS sample buffer. The elutes were analyzed by SDS-PAGE and western blot analysis using anti-Flag antibody.

Supplemental Figure Legends

Supplemental Figure 1:

Fritz expression pattern, morphant phenotypes, and protein localization. (A) *Fritz* expression in the dorsal mesoderm of a gastrulating *Xenopus* embryo. (B) Fritz mRNA is expressed in the midline and in a punctate pattern in the ciliated epidermis (arrows). (C) Fritz is expressed in the otic vesicle (blue arrowhead) and the nephrostomes (red arrowheads). (D) Fritz is expressed in the otic vesicle (blue arrowhead) and the ventral neural tube (orange arrowhead). (E) Control embryos at tailbud stage. (F) Sibling Fritz morphant embryos with short axes and dorsal flexure. (G) Control Keller explants elongate normally. (H) Keller explants from Fritz morphants failed to elongate, demonstrating a requirement for Fritz specifically in convergent extension, rather than other morphogenetic processes of gastrulation such as head mesoderm migration, epiboly, or vegetal rotation (*4*). (I) Western blot showing loss of endogenous Fritz in morphants (lanes 2 and 3). (J) In multi-ciliated cells, Fritz protein is enriched in foci at the apical surface of multi-ciliated cells (mcc) and at the plasma membrane of the surrounding cells. (K) Co-immunostaining of the apical surface of multi-ciliated cells reveals that Fritz (green) localizes adjacent to the basal body, marked by γ-tubulin (red in k'). (L) Co-immunostaining reveals that Fritz decorates the axonemes in multi-ciliated cells, as marked by co-localization with α-tubulin (red in i').

Supplemental Figure 2: Collective cell movement (convergent extension) of dorsal mesoderm cells in organotypic culture. (A) Schematic outline of preparation and organotypic culture of dorsal marginal zone tissue from the *Xenopus* gastrula ("Keller explants"). (B) Schematic of tissue-level behavior of Keller explant in culture. (C) Schematic of cell behaviors in Keller explants; cells align and elongate mediolaterally and then interdigitate.

Supplemental Figure 3: Morphometrics of cells in gastrula and neurula stage Keller explants. (A) Images show still frames from time-lapse movies of gastrula mesoderm in organotypic culture. Green arrows indicate cells with long axis oriented mediolaterally; red arrow indicate cells with long axis oriented anteroposterior. Orientation of cells from several explants per condition are plotted in rose diagrams below. The matrix shows p values for chi square test between the conditions. Control, Fritz-MO and Sept2-MO are not significantly different; Xdd1 is significantly different from all other conditions. (B) Graph of length-to-width ratio for gastrula mesoderm cells. The matrix shows p values for Kruskal-Wallis tests between the conditions. N= 127 cells (control), 176 cells (Xdd1), 40 cells (Fritz-MO), 59 cells (Sept2-MO).

Supplemental Figure 4: Expression of Septins. Upper panels show sept2 and sept7 expression in the mesoderm in sagittal sections of mid-gastrula stages (dorsal at right). Middle panels show sept2 and sept7 expression in the mesoderm in vegetal views of intact embryos later in gastrulation (dorsal at top). Lower panels show sept2 and sept7 expression in the notochord (NC) in transverse sections of neurula stage embryos (dorsal at top).

Supplemental Figure 5: Sept2 and Sept7 morphants display similar cell behavior phenotypes during convergent extension. (A) Still image from time-lapse movie of dorsal mesoderm cells in a sept7 morphant Keller explant (compare to Sept2 MO in Fig. 1O); yellow lines indicate positions of kymographs shown in a' and a''.

Supplemental Figure 6: Phycial interaction between Fritz and Septin. (A) Sept2-GFP is co-immunoprecipitated by myc-Fritz, but GFP alone is not. (B) Flag-Fritz is co-immunoprecipitated by myc-sept2.

Supplemental Figure 7: Quantification of defects in Sept7 foci in multi-ciliated cells of Fritz morphants. (A) Reduction of mean area of foci. (B) Increase in pixel heterogeneity of foci. N = 299 control foci; 185 morphant foci.

Supplemental Figure 8: Fritz controls distribution of sept2 in multi-ciliated cells (A) Control multi-ciliated cell covered with a dense tuft of cilia. (B) Z-projection of the cell in A; separation of channels reveal localization of myc-tagged sept2 (green in b') in the axoneme (marked by tubulin, red in c''). Little or no sept2 signal is apparent in the cytoplasm. (C) Fritz morphant cell with few cilia. (D) Z-projection

of the cell in C; separation of channels reveals that myc-tagged sept2 signal accumulates aberrantly in the cytoplasm of Fritz morphant.

(E) Control multi-ciliated cells in the *Xenopus* epidermis. (F) Cilia are disrupted in sept2 morphant (G) Sagittal view the Hedgehog target gene *Nkx2.2* in the spinal cord of a control embryo marked by black arrowheads. (H) *Nkx2.2* expression is lost in sept2 morphant embryo marked by red arrowheads.

Supplemental Figure 9. Knockdown of Septins does not affect expression of the Notch target Hrt1 in the ventral neural tube. (A) Control (B) Sept2 morphant. (C) Sept 7 morphant.

Supplemental Figure 10. Fritz residues mutated in human ciliopathy patients. (A) Primary sequence alignment of regions containing Fritz (C2ORF86) mutations in human patients. (B) Predicted structure of human Fritz. The Fritz sequence threads well against many WD-repeat β-propeller proteins. Shown here is the model based on human WDR39 (3fm0). (C) Positions of the R55 and L208 residues in the Fritz protein, which are mutated in human patients, are shown in red on a model of the Fritz structure based on yeast NUP159 (1xip). (D) Pedigree showing segregation of a homozygous splice mutation in Fritz with the BBS disease phenotype.

Supplemental Movie Legends

Supplemental Movie 1: Time-lapse movie of cells in a representative Keller explant taken from a control embryo.

Supplemental Movie 2: Time-lapse movie of cells in a representative Keller explant taken from a Fritz morphant embryo.

Supplemental Movie 3: Time-lapse movie of cells in a representative Keller explant taken from a sept2 morphant embryo.

Supplemental Movie 4: Time-lapse movie of cells in a representative Keller explant taken from a sept7 morphant embryo.

References:

1. H. L. Sive, R. M. Grainger, R. M. Harland, *Early Development of Xenopus laevis: A Laboratory Manual*. (Cold Spring Harbor Press, Cold Spring Harbor, N.Y., 2000).
2. S. A. Moody, M. J. Kline, *Anat. Embryol. (Berl).* **182**, 347 (1990).
3. C. J. Lee, K. E.K., R. S. Gray, T. J. Park, J. B. Wallingford, *Cold Spring Harbor Protocols*, (2008).
4. R. Keller, L. A. Davidson, D. R. Shook, *Differentiation* **71**, 171 (Apr, 2003).

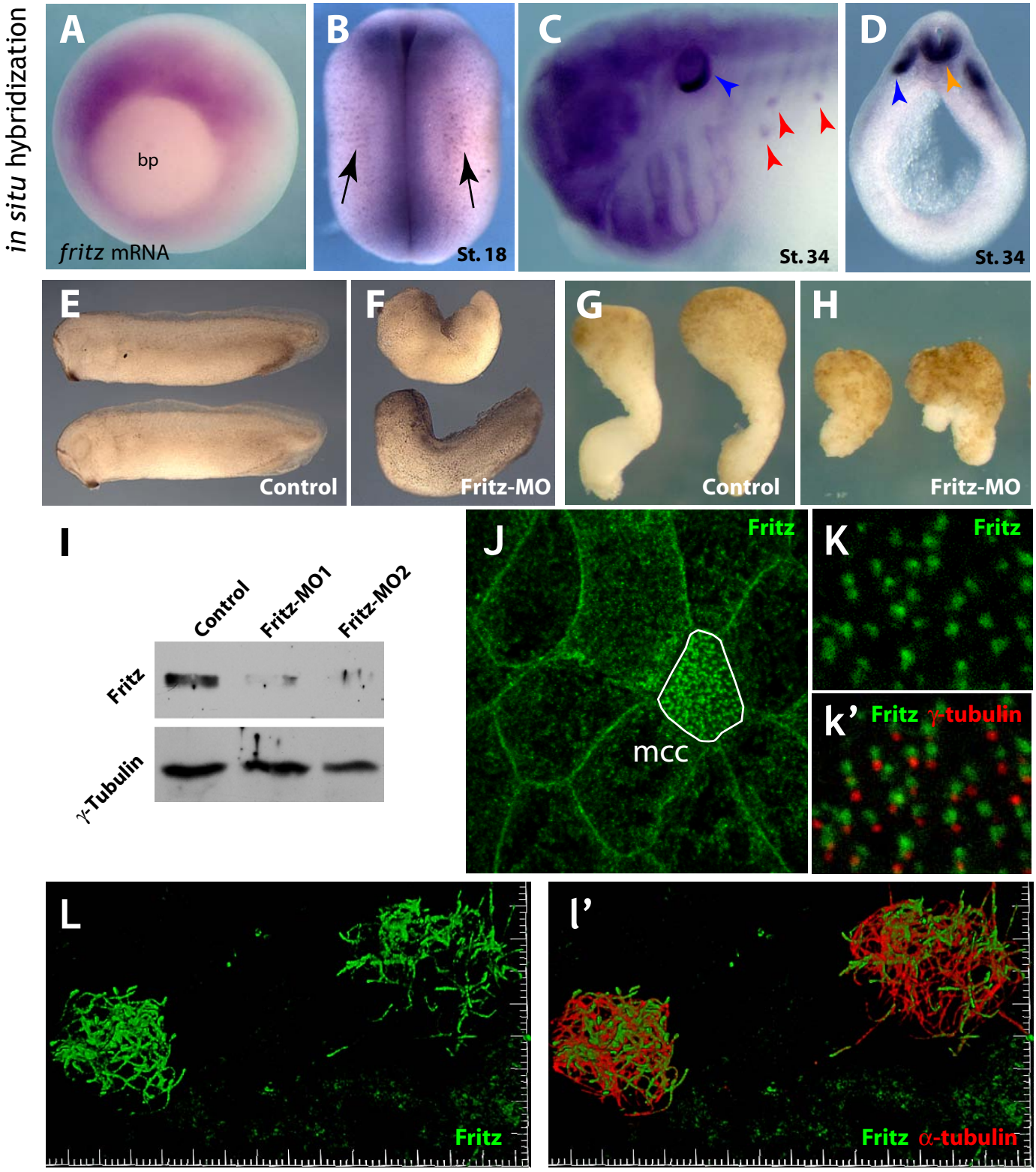

Supplemental Figure 1
Kim et al.

A. Preparation and imaging of cultured organotypic explants of dorsal gastrula mesoderm ("Keller" explants)

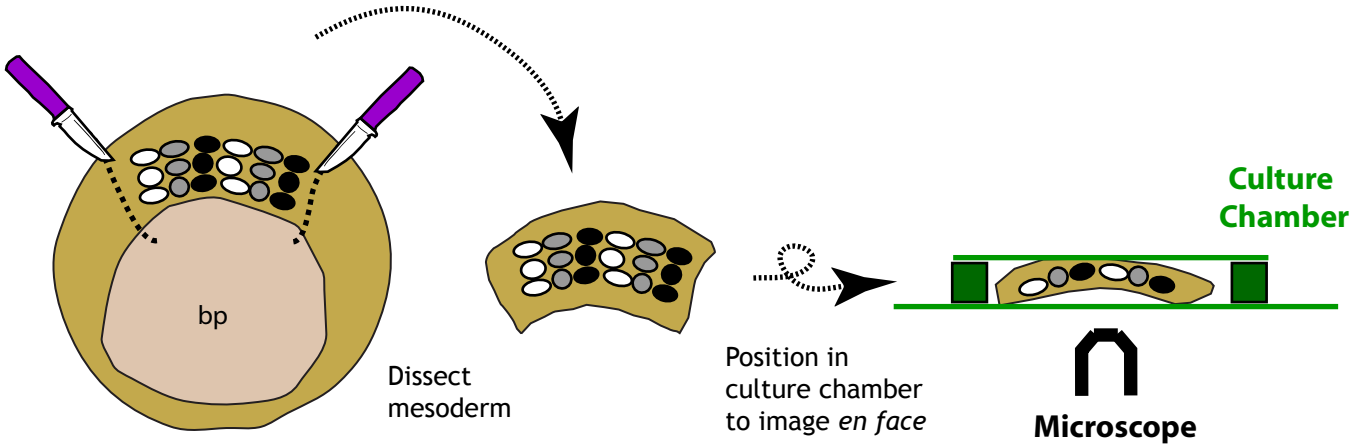

B. Tissue movement during convergent extension

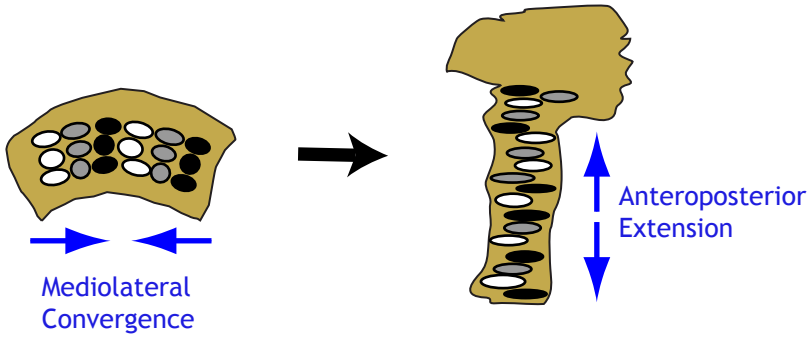

C. Cell behavior during convergent extension

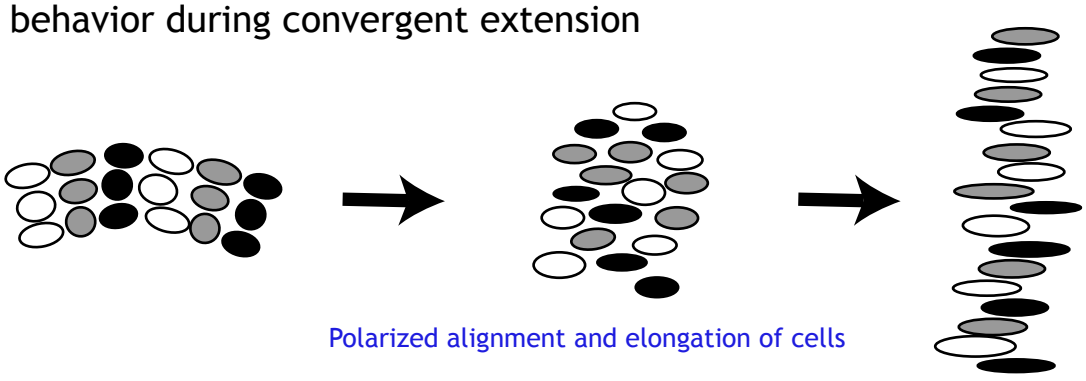

Supplemental Figure 2
Kim et al.

A

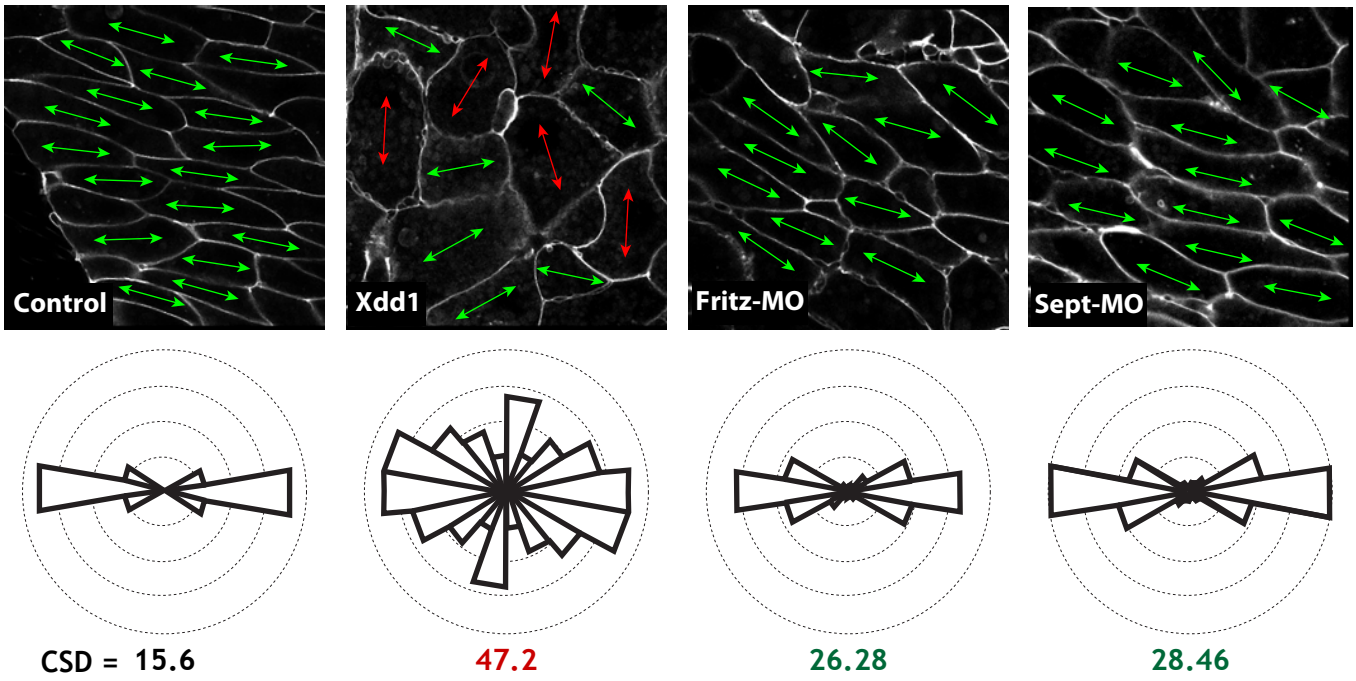

Circular standard deviation p values

(Chi Square, class width = 15°)

	Fritz-MO	Sept2-MO	Xdd1
Ctl	0.068	0.069	<0.01
Fritz-MO	----	0.95	<0.01
Sept2-MO		----	<0.01

B

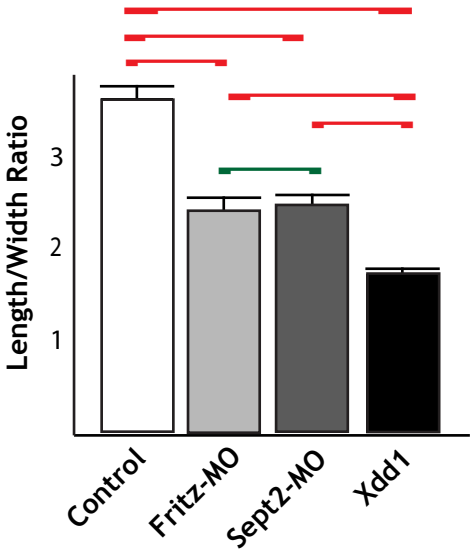

Length/Width Ratio p values

(Kruskal-Wallis test)

	Fritz-MO	Sept2-MO	Xdd1
Ctl	<0.01	<0.01	<0.01
Fritz-MO	----	>0.05	<0.01
Sept2-MO		----	<0.01

Supplemental Figure 3
Kim et al.

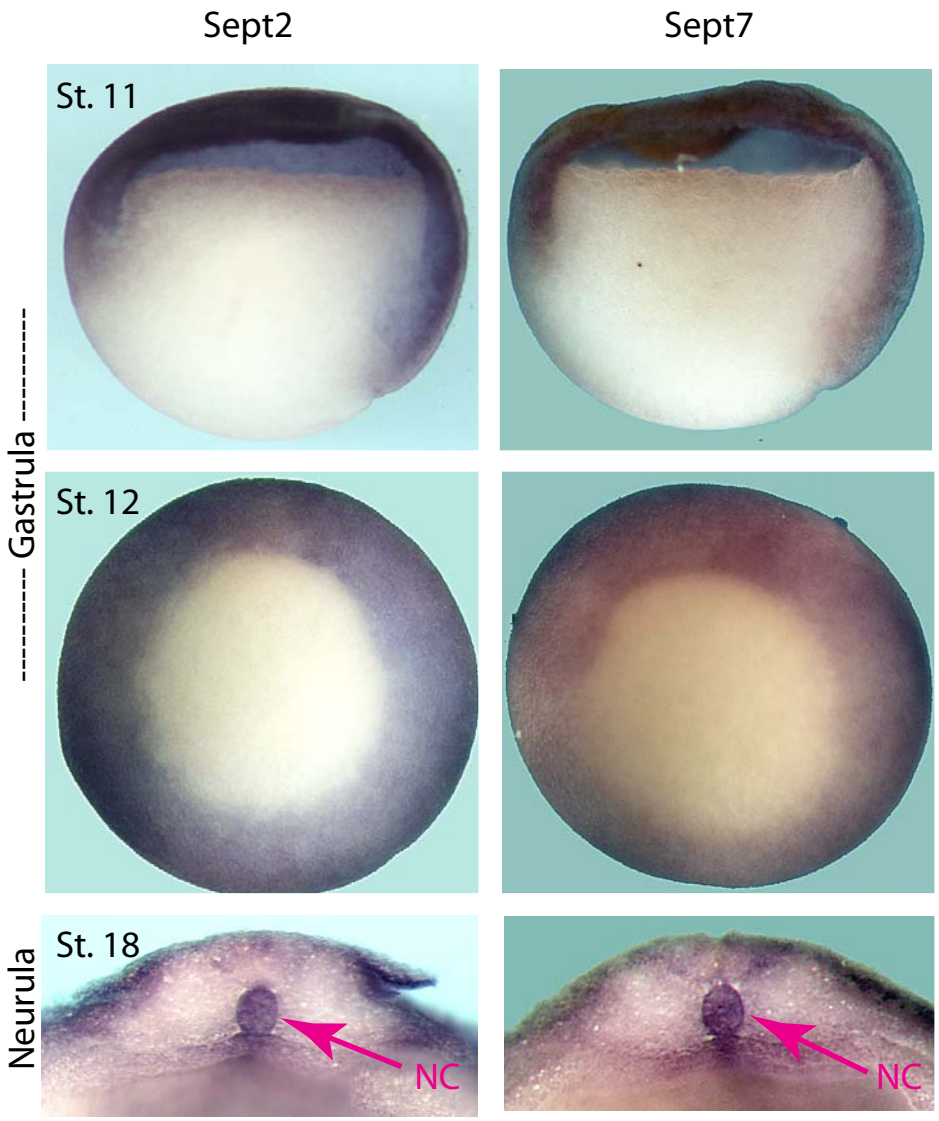

Supplemental Figure 4
Kim et al.

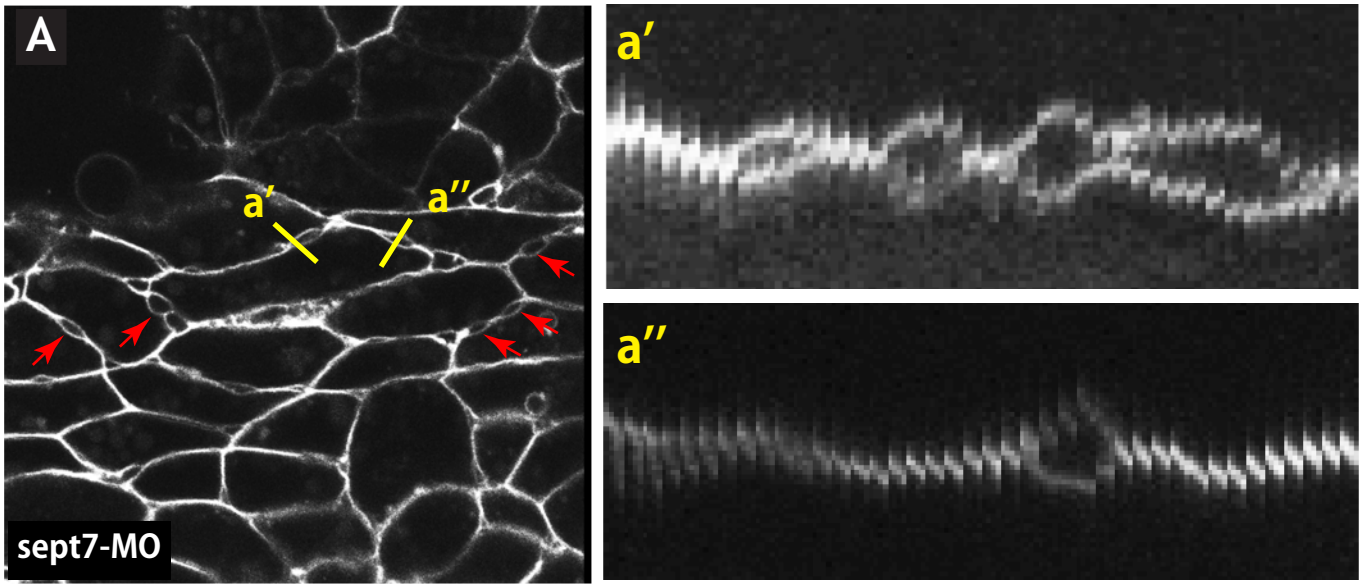

Supplemental Figure 5
Kim et al.

A

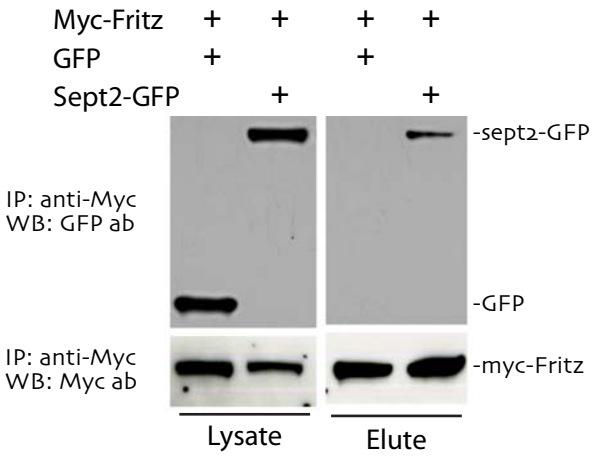

B

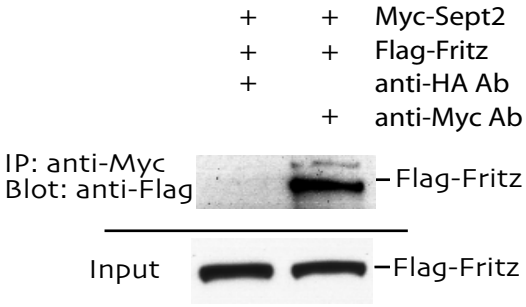

Supplemental Figure 6
Kim et al.

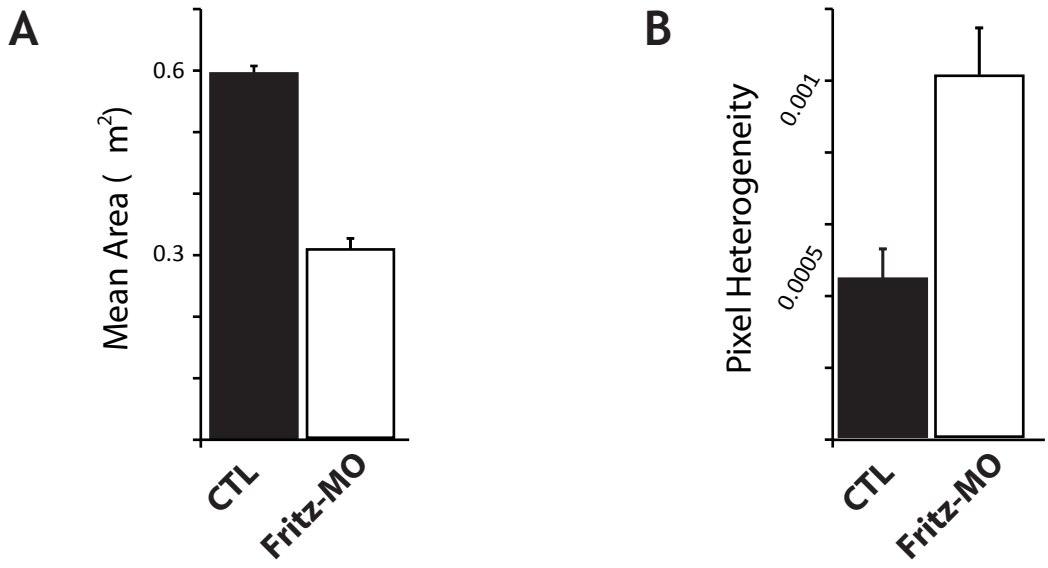

Supplemental Figure 7
Kim et al.

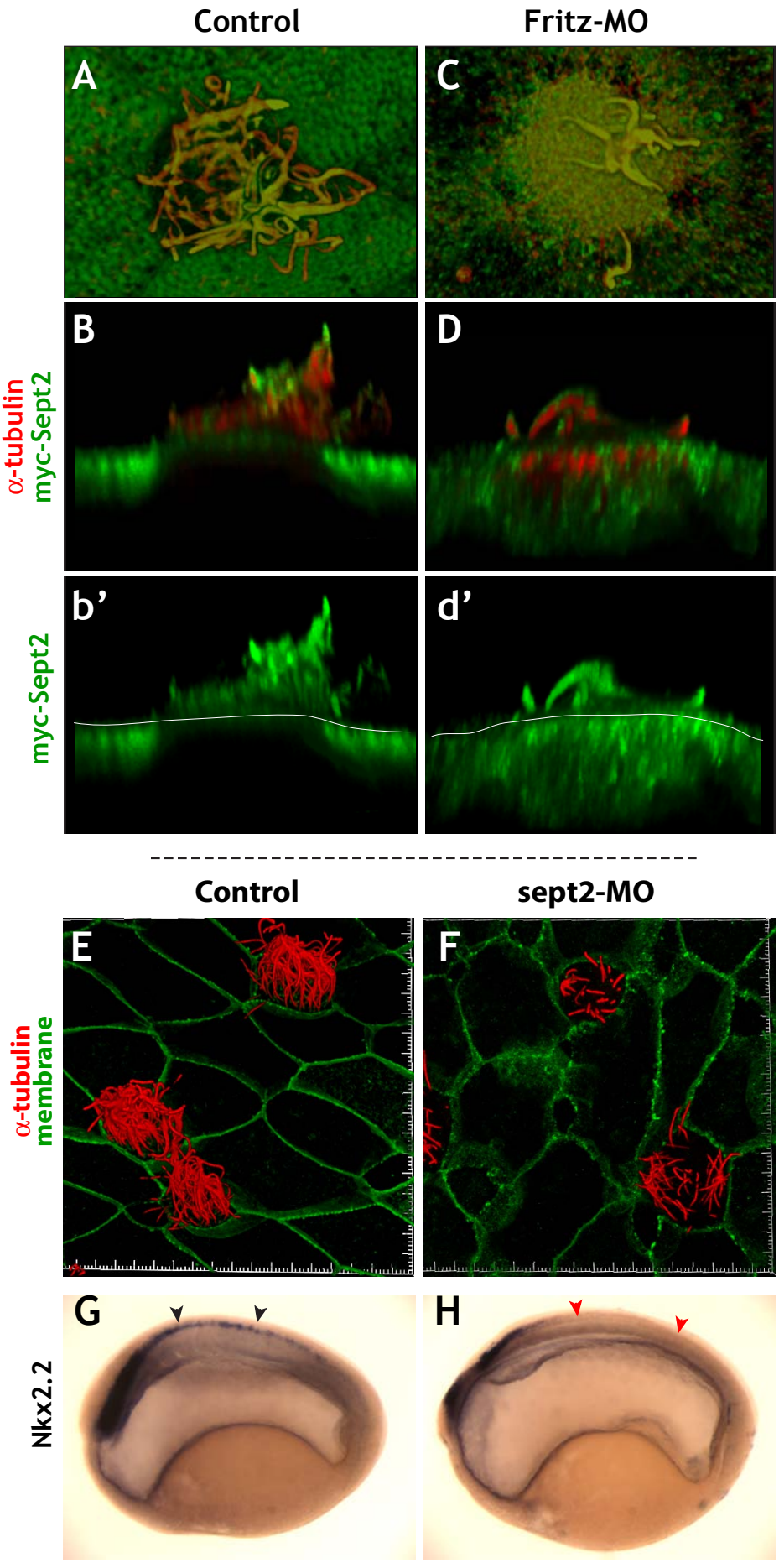

Supplemental Figure 8
Kim et al.

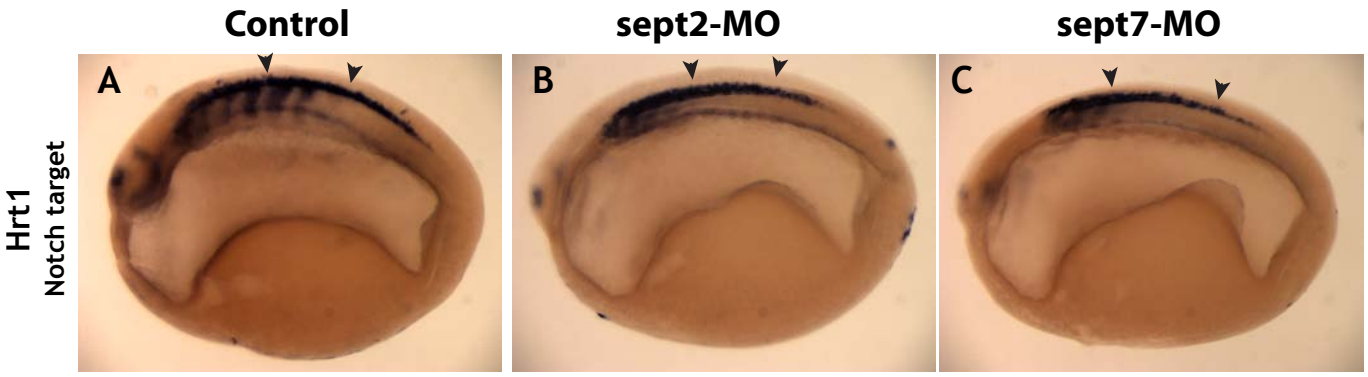

Supplemental Figure 9
Kim et al.

A

R55K

Human	D	R	D	I	G	I	Y	Q	Y	Y
Rhesus	D	R	N	I	G	I	Y	Q	Y	Y
Mouse	D	R	D	I	G	V	Y	Q	Y	Y
Dog	D	R	D	I	G	I	Y	Q	Y	Y
Elephant	D	R	D	I	G	T	Y	Q	Y	Y
Opossum	D	R	D	I	G	I	Y	Q	Y	Y
Chicken	D	E	D	I	G	V	H	Q	Y	Y
Xenopus	D	E	D	V	G	V	H	Q	Y	Y

L208F

Human	R	L	E	K	L	S	A	L	D	Y
Rhesus	R	L	E	K	L	S	A	L	D	Y
Mouse	R	L	E	K	L	S	A	L	D	L
Dog	R	L	E	K	L	S	A	L	D	Y
Elephant	R	F	E	K	L	S	A	L	D	Y
Opossum	R	H	E	K	L	S	N	S	E	Y
Chicken	R	L	E	K	L	S	C	L	D	F
Xenopus	Q	L	E	K	L	S	L	L	D	L

S708F

Human	E	K	D	I	C	S	G	F	L	M
Rhesus	E	K	D	I	C	S	G	F	L	M
Mouse	E	E	E	V	C	T	D	S	S	G
Dog	E	K	D	T	R	A	E	S	L	M
Elephant	E	K	D	I	G	P	G	S	L	M
Opossum	E	K	D	I	Y	T	S	P	S	M

B

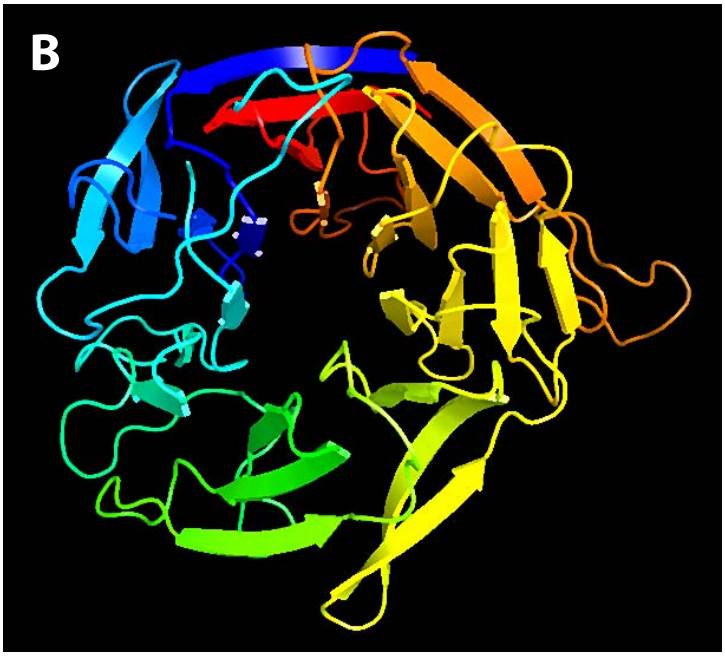

C

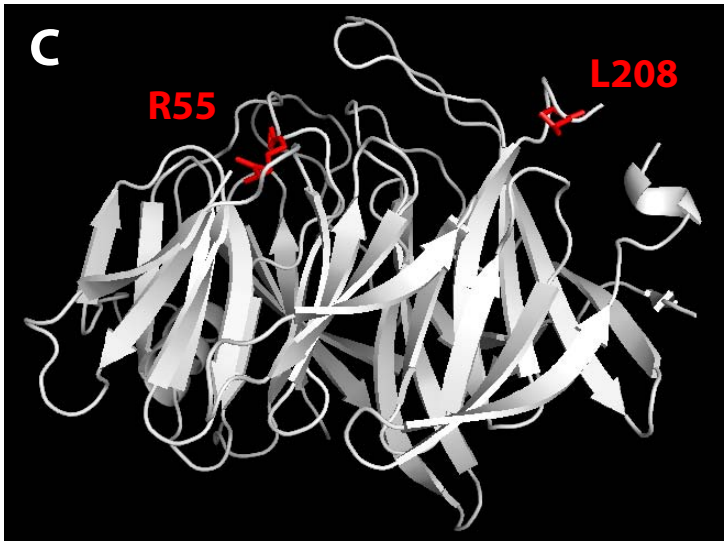

D

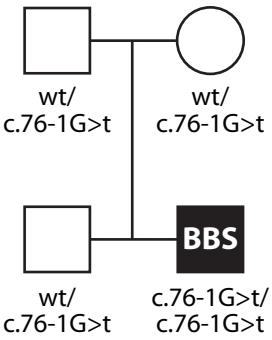

Supplemental Figure 10
Kim et al.